Prabitha Urwyler[a], Xue Zhao[b], Alfons Pascual, Helmut Schift and Bert Müller*

Tailoring surface nanostructures on polyaryletherketones for load-bearing implants

Abstract: High-performance thermoplastics including polyetheretherketone (PEEK) are key biomaterials for load-bearing implants. Plasma treatment of implants surfaces has been shown to chemically activate its surface, which is a prerequisite to achieve proper cell attachment. Oxygen plasma treatment of PEEK films results in very reproducible surface nanostructures and has been reported in the literature. Our goal is to apply the plasma treatment to another promising polymer, polyetherketoneketone (PEKK), and compare its characteristics to the ones of PEEK. Oxygen plasma treatments of plasma powers between 25 and 150 W were applied on 60 μm-thick PEKK and 100 μm-thick PEEK films. Analysis of the nanostructures by atomic force microscopy showed that the roughness increased and island density decreased with plasma power for both PEKK and PEEK films correlating with contact angle values without affecting bulk properties of the used films. Thermal analysis of the plasma-treated films shows that the plasma treatment does not change the bulk properties of the PEKK and PEEK films.

Keywords: Polyetheretherketone (PEEK); polyetherketoneketone (PEKK); oxygen plasma treatment; atomic force microscopy; differential scanning calorimetry.

[a]Present address: University of Bern, Gerontechnology and Rehabilitation group, 3010 Bern, Switzerland.
[b]Present address: EMPA, Laboratory for Nanoscale Materials Science, 8600 Dübendorf, Switzerland.
*Corresponding author: Bert Müller, Biomaterials Science Center (BMC), University of Basel, c/o University Hospital Basel, 4031 Basel, Switzerland, Phone: +41 61 265 9660, Fax: +41 61 265 9699, E-mail: bert.mueller@unibas.ch
Prabitha Urwyler: Biomaterials Science Center (BMC), University of Basel, c/o University Hospital Basel, 4031 Basel, Switzerland; and Paul Scherrer Institute (PSI), Laboratory for Micro- and Nanotechnology, 5232 Villigen PSI, Switzerland
Xue Zhao: Biomaterials Science Center (BMC), University of Basel, c/o University Hospital Basel, 4031 Basel, Switzerland
Alfons Pascual: University of Applied Sciences Northwestern Switzerland FHNW, Institute of Polymer Engineering (IKT), 5210 Windisch, Switzerland
Helmut Schift: Paul Scherrer Institute (PSI), Laboratory for Micro- and Nanotechnology, 5232 Villigen PSI, Switzerland

Introduction

Polyaryletherketones are semi-crystalline thermoplastics, which are thermally stable up to at least 250°C and exhibit high mechanical strengths compared to other polymers. While polyetheretherketone (PEEK) has been established as a high-performance polymer in the orthopedics (1, 2) and further medical implants (1, 3–6), polyetherketoneketone (PEKK) is only at the transition to medical applications. The structure of PEKK and PEEK, reproduced in Figure 1, is very similar. Both polymers, PEKK and PEEK, belong to the polyaryletherketone family, where benzene rings are linked via ether and ketone groups. The ratio and sequence of ethers to ketones affect the thermal properties including glass transition temperature, melting point, heat resistance, and processing temperature of the polymer. PEKK has a higher ratio of ketones than PEEK making the polymer chain more rigid. As a consequence, the reported glass transition temperature of PEKK (T_g=162°C) and the melting point of PEKK (T_m=395°) (7, 8) are significantly higher than the ones of PEEK (T_g=143°C, T_m=343°C) (9). In comparison to PEEK, PEKK has an extremely slow rate of crystallization leading to improved flow characteristics, lower mold-in stresses, and greater dimensional stability (10). PEKK also exhibits lower melt viscosity than PEEK (11) rendering easier processing of injection-molded products. Even more important for load-bearing implants are the mechanical properties of PEKK with respect to the established PEEK. The compressive yield strength of PEKK (205 MPa), for example, is twice as large as the one of PEEK (118 MPa). The density of PEKK (1.3 g/cm³) and of PEEK (1.3 g/cm³) (9) is closer to bone (1.9 g/cm³) (12) than that of the metals in use for load-bearing implants.

The thermo-mechanical properties of PEKK superior to the ones of PEEK are a clear advantage when working with thin film or thin-walled products. Nevertheless, as PEEK, PEKK is radiolucent, compatible to magnetic resonance imaging and chemically inert and, therefore, qualifies as a promising biomaterial for a variety of medical implants.

Several manufacturing processes including injecting molding are in use to produce medical implants from PEEK (13, 14). For osteointegration, the PEEK surfaces
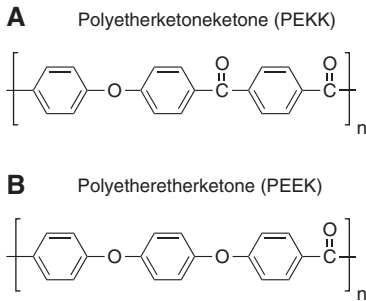
A   Polyetherketoneketone (PEKK)

B   Polyetheretherketone (PEEK)

Figure 1 Structure of PEKK and PEEK.

have to be activated to allow for proper cell attachment. The surface chemistry and roughness (15) play a crucial role in the biocompatibility of medical implants (16, 17) because adherent cells interact via dedicated proteins with the accessible micro- and nanostructures (18–20). Plasma treatment is a promising method because of the ease of the process and the reproducible control of the final surface chemistry. Plasma-based surface activation methods are also applied to fabricate vascular implants (21, 22).

Load-bearing implants made of titanium are sandblasted and etched to obtain the micro- and nanometer-scale roughness for osseointegration. In order to reach osseointegration for polymers and extend the applications beyond spinal disc cages and housings of pacemakers (1) the necessary roughness has to be generated. It has been shown that plasma treatments do not only chemically activate the polymer surfaces but also induce etching processes, which result in well-defined nanostructures (23, 24). The density and size of the nanostructures can be tailored by the choice of the process gas, the plasma power, and the duration of the plasma treatment. Very recently, it has been demonstrated (25, 26) that adipose tissue-derived mesenchymal stem cells seeded on plasma-treated PEEK films show an increased adhesion, a higher degree of proliferation, and an improved osteogenic differentiation compared to untreated films. When these cells were grown on films treated with 10 and 50 W oxygen and ammonia plasmas for a duration of 5 min, they exhibited a doubled mineralization degree relative to the untreated PEEK. As the plasma-treated PEEK films supported the osteogenic differentiation of stem cells in vitro, one can reasonably assume that plasma-treated PEEK implants holds perspective for suitable osseointegration of load-bearing PEEK implants in vivo.

We hypothesize that the oxygen plasma treatment can successfully be applied to PEKK films in a similar manner as to PEEK in order to realize nanostructures for improved osseointegration. In this communication, we apply the

methodology developed (23, 25) for both PEEK and PEKK films to present a detailed comparison of the two polymer biomaterials.

Materials and methods

Materials

Commercially available 100 µm-thick amorphous PEEK films (APTIV™ 2000 series, Victrex Europa GmbH, Hofheim, Germany) and 60 µm-thick PEKK films (OXPEKK Permetta™, Oxford Performance Materials, South Windsor, CT, USA) were used for this study. These commercially available PEKK films are only available with a nominal thickness of 60 µm, whereas PEEK films are offered with nominal thicknesses of 6, 12, 25, 50, 100, 200, and 300 µm. Our study is based on 100 µm-thick PEEK films because of the available data from previous research activities (23, 25).

PEEK sheet pretreatment by hot embossing

The 60 µm-thick PEKK and 100 µm-thick PEEK films were flattened by placing them between two polished, 500 µm-thick 4-inch Si(100) wafers (Si-Mat, Kaufenring, Germany) in a precision hot press (HEX03, Jenoptik AG, Jena, Germany), heated slightly above the glass transition temperatures under a pressure of 40 kN for a period of 10 min and subsequently cooled down to room temperature with an average rate of 0.26 K/s. Hot embossing is meaningful as the viscous behavior of the thermoplastic polyaryletherketones allows flattening the surface undulations including scratches with a polished Si wafer, which exhibits a roughness well below 2 nm. The thicknesses of the original and embossed films were measured using a micrometer gauge (115151 digital FUTURO IP65, Brütsch/Rüegger Tools Ltd, Urdorf, Switzerland) with a resolution of 1 µm. The measured thicknesses of the commercially available films were (82.0±2.0) µm for the nominally 60 µm-thick PEKK films and (98.5±1.5) µm for the nominally 100 µm-thick PEEK films. After embossing, the thicknesses were determined to (76.4±2.0) µm for PEKK and (94.4±0.8) µm for PEEK films. This means that the hot embossing process did not only reduce the roughness but also the film thickness for PEKK and PEEK by about 6 µm each.

Surface nanopatterning by plasma treatment

Oxygen plasma treatments (RIE System Plasmalab 80 Plus, Oxford Instruments, Yatton, UK) activated the original and embossed PEKK and PEEK films, respectively. The films were placed at the bottom-center of the plasma chamber. Subsequently, the chamber was evacuated, flushed for a period of 5 min with oxygen/argon (100/50 sccm) and then equilibrated for further 5 min with oxygen/argon (20/10 sccm). The plasma treatments with a duration of 5 min using a power between 25 and 150 W for the PEKK films and between 25 and 100 W for the PEEK films resulted in pressures between 25 and 98 mTorr and DC bias voltages between 146 and 372 V.

Surface topography measurements by atomic force microscopy (AFM)

AFM measurements enabled us to determine the roughness of plasma-activated PEKK and PEEK surfaces. The measurements were performed in Tapping Mode® in ambient air under dry conditions on a Dimension™ 3100 instrument (Veeco, Mannheim, Germany) using silicon cantilevers with Si_3N_4 coating and a tip radius of 20 nm, a spring constant of 40 N/m and a resonance frequency of 325 kHz (NSC15/A1BS, Mikromasch, CA, USA). Tips with a radius smaller than 20 nm may provide more details of the plasma-induced nanostructures. The scan area was set to 2×2 μm² and 1×1 μm², respectively. The data processing and the roughness evaluation were performed using the Nanoscope 6.13R1 software (Veeco Instruments Inc., Santa Barbara, CA, USA).

Island density measurement by scanning electron microscopy

The plasma-treated PEKK and PEEK films were coated with Cr using a current of 20 mA and applied a vacuum of 6 Pa (sputter coater Polaron, Thermo VG Scientific, Germany) during a period of 30 s. The surface structures were investigated with the field emission scanning electron microscope (SEM) Supra 40 VP (Carl Zeiss, Jena, Germany) with an electron energy of 2 keV using the InLens detector at a working distance (WD) of 6.8 mm. For each specimen the island density was determined from four characteristic square areas each containing approximately 150 islands.

Water contact angle measurements

The wettability of the plasma-treated PEKK and PEEK films and their controls was determined with double distilled water (ddH$_2$O) by the sessile drop contact angle method using a contact angle goniometer (Drop Shape Analysis System PSA 10 Mk2, Krüss, Hamburg, Germany). Contact angles were measured in triplicate 5 s after placing a 4 μL water droplet at room temperature.

Thermal analysis by differential scanning calorimetry (DSC)

For the thermal analysis, the PEKK and PEEK films with a mass of about 2 mg were encapsulated in a standard sample pan of aluminum to acquire differential scanning calorimeter (DSCQ1000, TA Instruments, Waters GmbH, Eschborn, Germany) data. The complete protocol, consisting of a first heating cycle from 40 to 400°C, subsequent cooling to 40°C and a second heating cycle again to 400°C, was conducted in a dry N_2-atmosphere. The heating and cooling rates were set to 10 K per minute.

Results

Oxygen plasma treatments etch the surface of PEKK films in a similar manner as known from PEEK films. The plasma treatment with a duration of 5 min and a plasma power between 25 and 150 W results in nanostructures of increasing size and gives rise to polymer surfaces with increasing roughness as represented by a series of AFM images for PEKK and PEEK, respectively, in Figure 2.

The generated nanostructures can be tuned controlling the plasma power. This observation is valid for both the original and the embossed PEKK films as demonstrated by the series of AFM images and Figure 3.

The root-mean-square (RMS) roughness derived from the AFM measurements of the PEKK and PEEK films as supplied corresponded to 7.1 and 7.0 nm, respectively, using a scanning range of (2 μm)². The scanning range has prominent impact. For a scanning range of (1 μm)² the derived RMS roughness values corresponded to 3.9 nm for the PEKK and 2.3 nm for the PEEK films. After the hot embossing the RMS roughness of the films was reduced to 2.2 and 1.0 nm for PEKK and 0.5 and 0.5 nm for PEEK considering scanning ranges of (2 μm)² and (1 μm)², respectively. The RMS roughness of the polymer films increases with the plasma power as shown in Figure 4A and are equal for the original and the embossed films within the error bars. Therefore, the data displayed in Figure 4 are averaged values of the data from the original and the embossed polymer films.
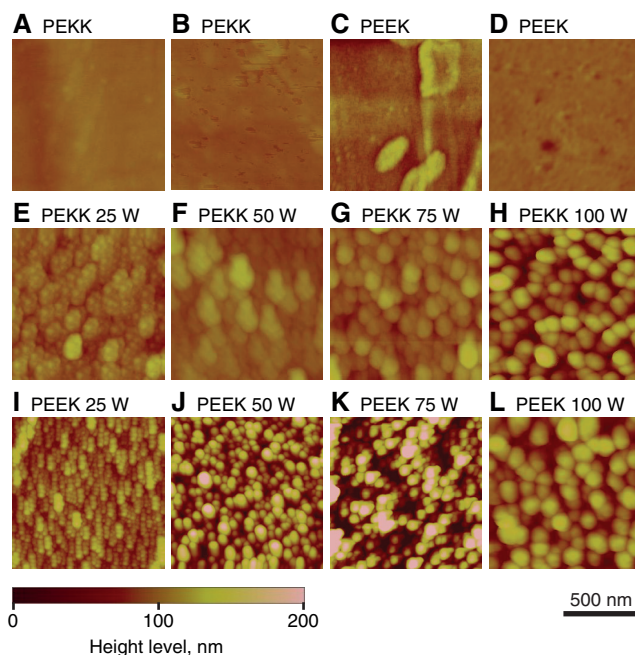

Figure 2 AFM images of the untreated, original and embossed PEKK (A,B) and PEEK (C,D) films as well as the embossed and oxygen plasma treated PEKK (E-H) and PEEK (I–L) films. The plasma power applied for 5 min and the employed polymer are indicated above each image. The height of the islands is color-coded. The AFM images represented have a size of 1 μm×1 μm.
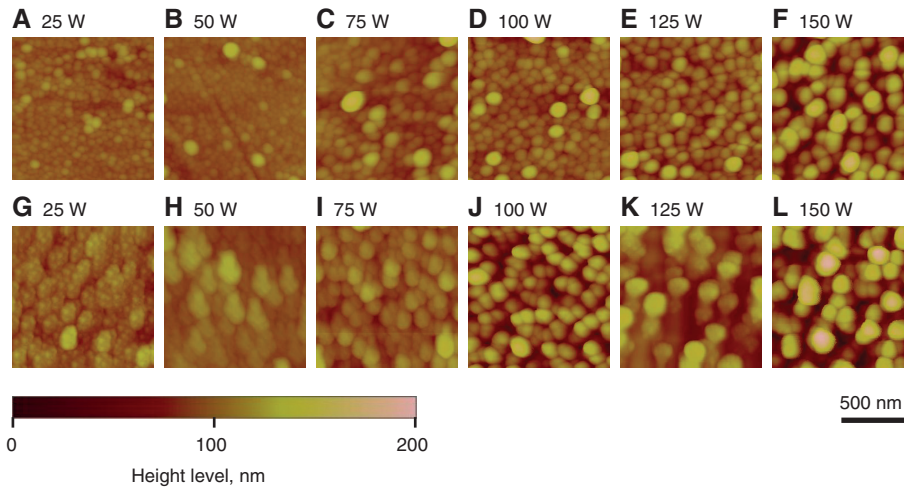
Figure 3 AFM images of PEKK films plasma-treated before (A-F) and after embossing (G-L). The plasma power is indicated above each AFM image.
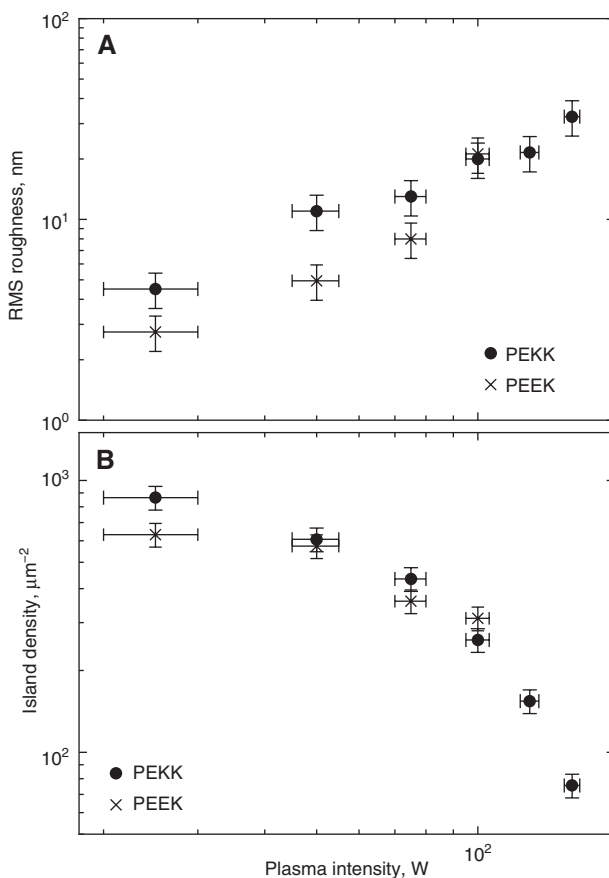

Figure 4 RMS roughness (A) and island density (B) of plasma-treated PEKK and PEEK films. The data shown are average values obtained from the AFM images and SEM images, respectively, of original and embossed polymer films.

The island densities derived from SEM images (images not shown), see Figure 4B, decrease with plasma power for both PEKK and PEEK films. As the island density measurement is generally considered to be more reliable compared to the determination of the RMS roughness, one can conclude that there is no significant difference in the surface morphology of oxygen plasma-treated PEEK and PEKK. Nevertheless, one can find a tendency that PEKK exhibits a smaller RMS roughness and a larger island density for the treatments with a lower plasma power, a fact that seems to be contradictory.

Water contact angle measurements belong to the powerful characteristics in biomaterials research and development. This physico-chemical property does not only depend on the nanometer-scale roughness (15) but above all on the chemical composition of the biomaterials surface. For PEEK, it has been shown (23) that a contact angle of about 40° is beneficial. Therefore, a comparative investigation of the contact angles on plasma-treated PEKK and PEEK is highly desirable. Figure 5 shows that the water contact angle for PEKK and PEEK films decreases with the applied plasma power.

In contrast to the measurements of the surface morphology, there are significant differences between the water contact angles measured on PEEK and PEKK films. The water contact angle decreases as a function of the applied plasma power much more for the treated PEKK than for the treated PEEK films. The effect is more prominent for the embossed PEKK films, as shown in Figure 5 comparing the data in A and B.

As the mechanical properties of load-bearing implants mainly depend on the bulk properties and usually hardly on the surface chemistry and morphology, one has to identify potential modifications of the bulk characteristics as the result of plasma treatments and embossing. The results of DSC, summarized in Table 1 as well as in
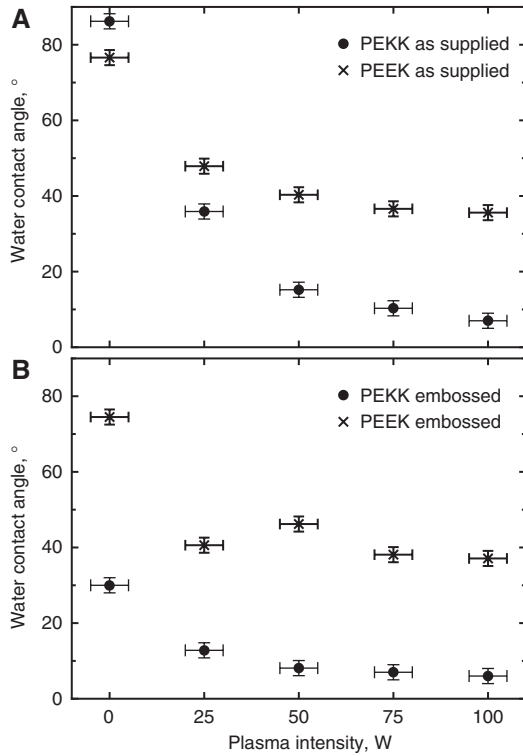
Figure 5 Water contact angle of plasma-treated PEKK and PEEK films. The term "as supplied" refers to the original films, which were not embossed.

above the glass transition temperature can influence the crystallinity and can have a significant impact on the mechanical properties of the polymer. Therefore, the DSC experiments were also performed with the embossed PEKK and PEEK films. These data given in Figure 7 demonstrate, however, that the embossing process used does not change the thermal properties of plasma-treated PEKK and PEEK.

Table 1 for PEKK and Table 2 for PEEK list the thermal characteristics derived from the DSC measurements. They do not only show that there is no difference between the original (as supplied) and the embossed films for the thermal quantities derived from DSC, but also indicate prominent differences for the first heating cycle.

The rather small endothermic peak, seen in the graphs of Figures 6B and 7B, denote the relaxation enthalpy, which accompanies the glass transition T_g and is similar for the applied plasma treatments. The endothermic peak observed in the graphs at a temperature of $(302\pm1)^\circ$C for PEKK and $(341.0\pm0.5)^\circ$C for PEEK indicates the melting temperatures T_m of the PEKK and PEEK films, respectively. These endothermic peaks give rise to a melting enthalpy $\Delta H_{m2}=(3.5\pm0.5)$ J/g for PEKK and a melting enthalpy $\Delta H_{m2}=(47\pm1)$ J/g for PEEK. The exothermic peak at a temperature of $(298\pm1)^\circ$C, see graphs in Figures 6D, 6E, 7D, and 7E, corresponds to the crystallization temperature T_c for PEEK. Here, we derived a cold crystallization enthalpy ΔH_c of (53 ± 1) J/g. The melting enthalpy and the cold crystallization enthalpy did not vary for the different plasma intensities for the original and the embossed PEEK films. Thus, the effect of the plasma treatment on the thermal properties PEEK films is negligible.

Figures 6 and 7, do not show any influence of the plasma treatment on the thermal properties of the PEKK films.

The thermal properties are closely related to the crystallinity of the polymer films. The embossing at temperatures

Table 1 Thermal properties of the plasma-treated PEKK films.

Plasma intensity, W	Embossed							As supplied						
	0	25	50	75	100	125	150	0	25	50	75	100	125	150
1st heating														
T_{g1}, °C	153	152	151	153	152	153	153	154	154	154	154	154	154	154
T_{k1}, °C	250	237	235	234	238	242	241	258	257	258	257	257	258	257
ΔH_{k1}, J/g	8	14	15	11	13	11	9	5	3	3	3	3	5	4
T_{m1}, °C	301	298	298	29	298	299	299	303	303	302	302	303	303	303
ΔH_{m1}, J/g	8	15	16	20	14	13	15	4	5	5	6	5	4	4
Cooling														
T_{gc}, °C				150.5±0.5							150.5±0.5			
2nd heating														
T_{g2}, °C				154.5±0.5							154.5±0.5			
T_{k2}, °C				260.0±2.0							260.0±2.0			
ΔH_{k2}, J/g				3±1							3±1			
T_{m2}, °C				302±1							302±1			
ΔH_{m2}, J/g				3.5±0.5							3.5±0.5			

T_m, melting temperature; T_k, crystallization temperature; T_c, cold crystallization temperature; T_g, glass transition temperature; ΔH_m, melting enthalpy; ΔH_k, crystallization enthalpy; ΔH_c, cold crystallization enthalpy.
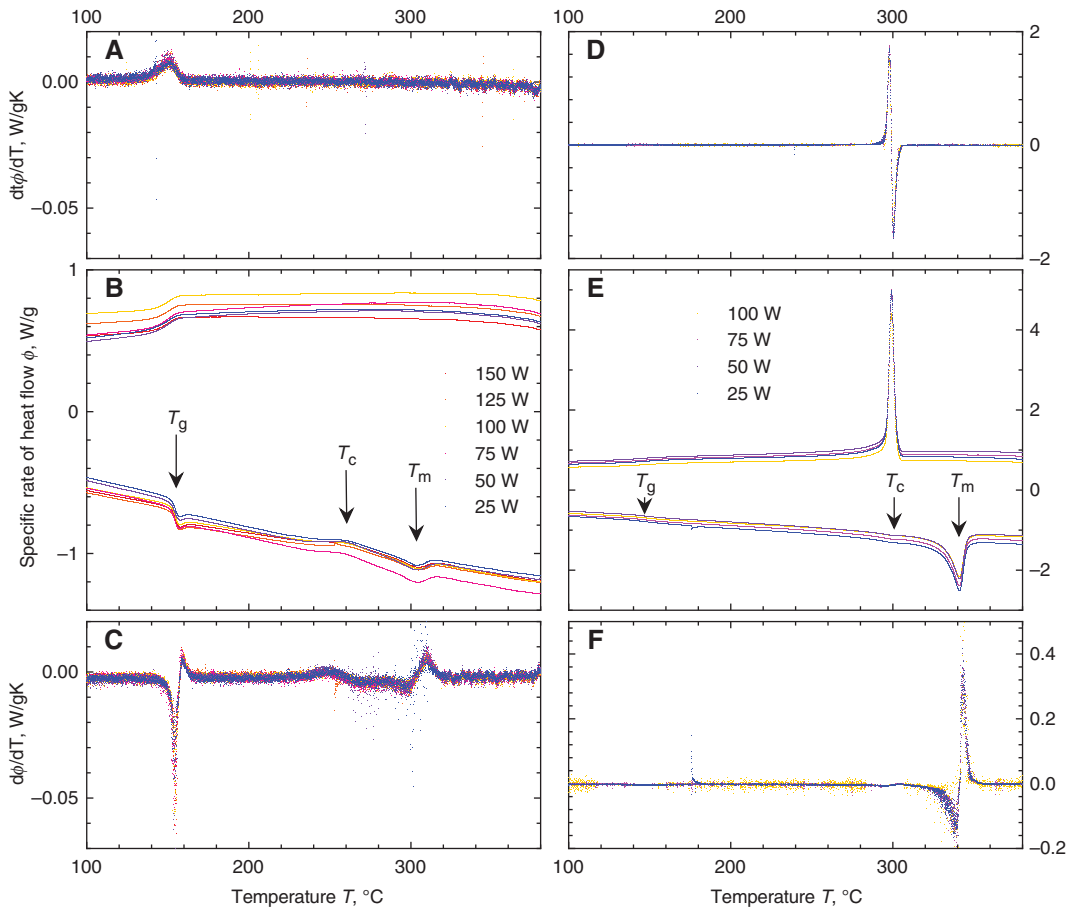
Figure 6 DSC analyses during cooling and second heating of original, non-embossed PEKK (A-C) and PEEK (D-F) films for the plasma powers indicated. The central part (B and E) shows close similarities between the curves obtained for the plasma-treated films, but does not allow distinguishing of curves with minor changes. Therefore, the differentiated curves of cooling are presented in A and D, respectively, and of the subsequent heating in C and F. These differentiated curves clearly demonstrate that the characteristic temperatures (melting temperature, cold crystallization temperature, glass transition temperature) are not affected for both plasma-treated PEKK and PEEK films.

We found, however, a strong difference between the embossed PEKK and PEEK films and their not embossed counterparts within the first heating cycle of the DSC measurement as summarized in Tables 1 and 2. This clear increase in the crystallinity, however, does not correlate with the applied plasma power.

Discussion and conclusions

Nanostructuring of polymers is an evolving field. Plasma-induced roughness on polymer surfaces has been known for a much longer period of time than a decade (27). While data of many polymers including PEEK (23) have been available, the results of plasma treatments on PEKK are unknown to the best of our knowledge.

PEEK and PEKK resemble not only with respect to their structure but exhibit very similar nanostructures after oxygen plasma treatment. The nanostructures on PEKK can be tailored by the choice of the plasma power as known from PEEK (24). Considering the surface morphology of PEKK and PEEK plasma-treated under equivalent conditions, it is difficult to identify any difference. Although the roughness of the plasma-treated surfaces is directly provided by the AFM system, the choice of the scanning speed and scanning range has an influence on the derived values. We selected a reasonably sized area of $2\,\mu m \times 2\,\mu m$ to obtain error bars that can be tolerated. SEM images of Cr-coated nanostructures served for the determination of the island density. The metal coating process using a sputter coater, a reactive process, may cause ramifications of the existing plasma-induced nanostructures. Thus, the error bars of the nanostructure density measurement were set to 10% although the counting is much more precise.

The water contact angle measurements accentuate the different surface properties of plasma-treated PEKK
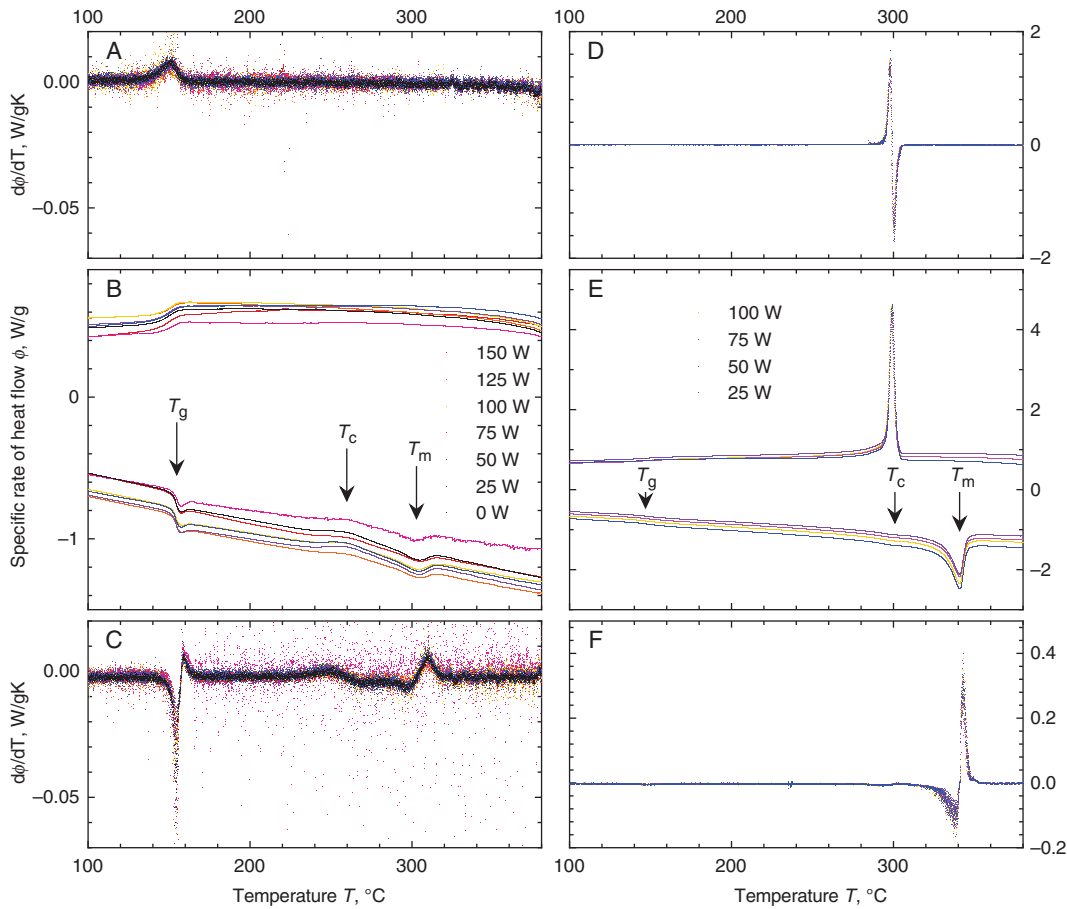
Figure 7 DSC analyses during cooling and second heating of the embossed PEKK (A-C) and PEEK (D-F) films for the plasma powers indicated. The central part (Panel B and Panel E) shows close similarities between the curves obtained for the plasma-treated films, but does not allow distinguishing of curves with minor changes. Therefore, the differentiated curves of cooling are presented in A and D and of the subsequent heating in C and F. These differentiated curves clearly demonstrate that the characteristic temperatures (melting temperature, cold crystallization temperature, glass transition temperature) are not affected for both embossed and plasma-treated PEKK and PEEK films.

Table 2 Thermal properties of plasma-treated PEEK films.

Plasma intensity, W	Embossed					As supplied				
	0	25	50	75	100	0	25	50	75	100
1st heating										
T_{g1}, °C	156	153	153	153	154	145	144	145	144	145
T_{k1}, °C	194	181	180	182	188	173	173	173	173	173
ΔH_{k1}, J/g	4	7	8	8	8	39	35	36	36	36
T_{m1}, °C	341	340	341	341	341	342	342	342	342	342
ΔH_{m1}, J/g	39	39	38	40	39	37	40	39	40	39
Cooling										
T_c, °C			298±1					298±1		
ΔH_c, J/g			53±1					53±1		
T_{gc}, °C			144±1					144±1		
2nd heating										
T_{g2}, °C			147±2					147±2		
T_{m2}, °C			341.0±0.5					341.0±0.5		
ΔH_{m2}, J/g			47±1					47±1		

T_m, melting temperature; T_k, crystallization temperature; T_c, cold crystallization temperature; T_g, glass transition temperature; ΔH_m, melting enthalpy; ΔH_k, crystallization enthalpy; ΔH_c, cold crystallization enthalpy.

and PEEK films. As the outcome of stem cell experiments favors substrates showing a contact angle of about 40° (25), PEKK films to be applied in cell and animal experiments should be plasma-treated with a power of 25 W. Additional process steps such as embossing should be avoided since they can give rise to water contact angles of significantly <20°. There are, however, studies related to other biomaterials (28–30), which favor water contact angles down to zero. As a consequence, PEKK might be even better suited for bone implants than PEEK.

The plasma treatments change the surface biocompatibility but do not significantly alter the bulk properties of PEKK and PEEK. Therefore, we can conclude that plasma treatments can be applied without influencing the mechanical properties of polyaryletherketone-based medical implants. Thermal treatments such as embossing with temperatures above T_g shift the implant towards the thermal equilibrium and thereby can modify the mechanical properties of PEEK and PEKK medical implants. Hence,

it might be advantageous to thermally treat the implants before the plasma treatment is carried out.

The PEKK and PEEK films were heated twice for the DSC study in order to destroy the thermal history. The thermal quantities, i.e. the glass transition temperature T_g and the melting temperature T_m, derived from the second heating cycle (cf. Tables 1 and 2) closely match to the values published in the related datasheets of PEKK (31) and PEEK (32) films.

In summary, the hypothesis that the oxygen plasma treatment allows the preparation of nanostructures on the surfaces of PEKK films in a similar manner as on the ones of PEEK (23, 25) is validated. The nanostructures that can be tailored by the choice of the plasma power are expected to improve the osseointegration of PEKK implants. These nanostructured PEKK implants are especially promising for bone implants in load-bearing applications.

References

1. Kurtz SM, Devine JN. PEEK biomaterials in trauma, orthopedic, and spinal implants. Biomaterials 2007;28:4845–69.
2. Knebel M. Titanium in difficulties. Kunstoffe 2010;2:68–71.
3. Jalbert F, Boetto S, Nadon F, Lauwers F, Schmidt E, Lopez R. One-step primary reconstruction for complex craniofacial resection with PEEK custom-made implants. J Craniomaxillofac Surg 2014;42:141–8.
4. Cook SD, Rust-Dawicki AM. Preliminary evaluation of titanium-coated PEEK dental implants. J Oral Implantol 1995;21:176–81.
5. Horak Z, Pokorny D, Fulin P, Slouf M, Jahoda D, Sosna A. [Polyetheretherketone (PEEK). Part I: prospects for use in orthopaedics and traumatology]. Acta Chir Orthop Traumatol Cech 2010;77:463–9.
6. Schwitalla A, Muller WD. PEEK dental implants: a review of the literature. J Oral Implantol 2013;39:743–9.
7. Mazur R, Botelho E, Costa M, Rezende M. Thermal and rheological evaluation of PEKK thermoplastic matrix for aeronautical application. Polímeros 2008;18:237–43.
8. Hsiao BS, Chang IY, Sauer BB. Isothermal crystallization kinetics of poly(ether ketone ketone) and its carbon-fibre-reinforced composites. Polymer 1991;32:2799–805.
9. Kurtz SM. PEEK Biomaterials Handbook. 1 ed. Oxford: Elsevier Science; 2011.
10. Precision Machining AIP. Materials-Plastics-PEKK (PolyEther-KetoneKetone) AIP Precision Machining; 2014 [cited 2014 02.09.2014]; Available from: http://aipprecision.com/en/materials/plastics/pekk.
11. Pilato LA, Michno MJ, editors. Advanced Composite Materials. Berlin: Springer; 1994.
12. Gong JK, Arnold JS, Cohn SH. Composition of Trabecular and Cortical Bone. Anat Rec 1964;149:325–31.
13. Poulsson AH, Eglin D, Zeiter S, Camenisch K, Sprecher C, Agarwal Y, et al. Osseointegration of machined, injection moulded and oxygen plasma modified PEEK implants in a sheep model. Biomaterials 2014;35:3717–28.
14. Yoo KM, Lee SW, Youn JR, Yoon DH, Cho YE, Yu J-P, et al. Injection molding of vertebral fixed cage implant. Fibers Polymers 2003;4:89–96.
15. Müller B, Riedel M, Michel R, Paul SM, Hofer R, Heger D, et al. Impact of nanometer-scale roughness on contact-angle hysteresis and globulin adsorption. J Vacuum Sci Technol B 2001;19:1715–20.
16. Anselme K, Ponche A, Bigerelle M. Relative influence of surface topography and surface chemistry on cell response to bone implant materials. Part 2: biological aspects. Proc Inst Mech Eng H 2010;224:1487–507.
17. Ponche A, Bigerelle M, Anselme K. Relative influence of surface topography and surface chemistry on cell response to bone implant materials. Part 1: physico-chemical effects. Proc Inst Mech Eng H 2010;224:1471–86.
18. Variola F, Brunski JB, Orsini G, Tambasco de Oliveira P, Wazen R, Nanci A. Nanoscale surface modifications of medically relevant metals: state-of-the art and perspectives. Nanoscale 2011;3:335–53.
19. Müller B. Natural Formation of nanostructures: from fundamentals in metal heteroepitaxy to applications in optics and biomaterials science. Surf Rev Lett 2001; 8:169–228.
20. Riedel M, Muller B, Wintermantel E. Protein adsorption and monocyte activation on germanium nanopyramids. Biomaterials 2001;22:2307–16.
21. Wise SG, Waterhouse A, Kondyurin A, Bilek MM, Weiss AS. Plasma-based biofunctionalization of vascular implants. Nanomedicine (Lond) 2012;7:1907–16.
22. Waterhouse A, Wise SG, Yin Y, Wu B, James B, Zreiqat H, et al. In vivo biocompatibility of a plasma-activated, coronary stent coating. Biomaterials 2012;33:7984–92.
23. Althaus J, Urwyler P, Padeste C, Heuberger R, Deyhle H, Schift H, et al. Micro- and nanostructured polymer substrates for biomedical applications. Proc Spie 2012;8339:83390Q.

24. Althaus J, Padeste C, Köser J, Pieles U, Peters K, Müller B. Nanostructuring polyetheretherketone for medical implants. Eur J Nanomed 2012;4:7–15.

25. Waser-Althaus J, Salamon A, Waser M, Padeste C, Kreutzer M, Pieles U, et al. Differentiation of human mesenchymal stem cells on plasma-treated polyethere-therketone. J Mater Sci 2014;25:515–25.

26. Morrison DS, Gadegaard N, Dalby MJ, Poulsson AH. The use of specific PEEK nanotopographies to modulate osteogenic behaviour in primary osteoprogenitor cells. Eur Cells Mater 2013;26:50.

27. Chan CM, Ko TM, Hiraoka H. Polymer surface modification by plasmas and photons. Surf Sci Rep 1996;24:1–54.

28. Hussain S. Textbook of Dental Materials. New Delhi: Jaypee Brothers Publishers; 2008.

29. Soratur. Essentials of Dental Materials. New Delhi: Jaypee Brothers Publishers; 2002.

30. Shalaby SW, Salz U. Polymers for Dental and Orthopedic Applications. Boca Raton, Florida: CRC Press; 2006.

31. OPM. High Performance Thermoplastic OXPEKK Permetta™ Film. 2009.

32. Victrex. APTIV 2000 Series Films. 2009.

Prabitha Urwyler received her Bachelor of Technology (B.Tech) in Computer Engineering from the Mangalore University, India in 1995. She worked as a software engineer at Melstar Information Technologies Ltd, India from 1995 to 1997 and later at the Swiss News Agency (SDA – ATS), Switzerland until 2008. She received her M.Sc in Biomedical Engineering from the University of Bern in 2008. In 2012, she completed her PhD degree in Biomedical Engineering on the fabrication, characterization and application of disposable micro-cantilevers for biomedical applications at the University of Basel and the Paul Scherrer Institut. She worked as a Postdoc at the Biomaterials Science Center, University of Basel from 2012 to 2013. She is currently working as a Postdocoral researcher at the Geron-technology and Rehabilitation group, University of Bern.
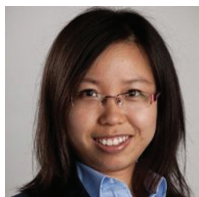
Xue Zhao studied physics in a joined Bachelor program of Wuhan University (China) and University Claude Bernard Lyon 1 (France), and received her BSc in Physics in 2010. She continued her studies in the department of physics at ETH Zürich, where she obtained her MSc in Physics in 2013. During this time she worked as intern at Paul Scherrer Institute and research assistant at University of Basel. Currently she is working towards her PhD in Experimental Physics on magnetism of coupled ferromagnetic and rare-earth ferromag-netic thin films at University of Basel and EMPA Dübendorf.

Alfons Pascual received his PhD in Organic Chemistry at the Sarriàs Chemical Institute (IQS, Barcelona University) in 1981 and worked on post-doc positions at the ETH in Zürich (Switzerland) and at the Max-Planck Institute in Mülheim a.d. Ruhr (Germany). From 1986 to 2000 he worked as laboratory head and project leader on design of insecticidal active compounds at Ciba-Geigy (from 1996 on Novartis) in Basel, Switzerland. Then he joined the University of Applied Sciences of Northwestern Switzerland (FHNW) as head of Polymer Analytics within the Institute of Polymer Engineering (IKT). He is strongly involved in failure analysis in polymeric materials.

Helmut Schift received his diploma in Electrical Engineering from the University of Karlsruhe, Germany. He performed his PhD studies at the Institute of Microtechnology Mainz (IMM), Germany. After his graduation in 1994, he joined PSI as a research staff member and is now head of the INKA-PSI Group in the Laboratory for Micro- and Nanotechnology at the PSI. He is actively involved in the development of nanoimprint lithography (NIL) as an alternative nanopatterning method for device fabrica-tion. He is currently working in various national and international projects on stamp fabrication, hybrid technologies and innovative 3-D nanomolding.

Bert Müller received a diploma in mechanical engineering (1982), followed by the MSc degree from the Dresden University of Technology and the PhD from the University of Hannover, Germany in 1989 and 1994. From 1994 to 2001, he worked as a researcher at the Paderborn University, Germany, EPF Lausanne, ETH Zurich. He became a faculty member of the Physics Department at ETH Zurich in April 2001. After his election as Thomas Straumann-Chair for Materials Science in Medicine at the University of Basel, Switzerland and his appointment at the Surgery Department of the University Hospital Basel in September 2006, he founded the Biomaterials Science Center. He also teaches physics and materials science at the ETH Zurich and the University of Basel.